Smart Electric Vehicle Charging Scheduler for Overloading Prevention of an Industry Client Power Distribution Transformer

Radu Godina[a], Eduardo M. G. Rodrigues[a], João C. O. Matias[a,b],
João P. S. Catalão [a,c,d],*

[a] *C-MAST, University of Beira Interior, R. Fonte do Lameiro, 6201-001 Covilhã, Portugal*
[b] *DEGEIT, University of Aveiro, Campus Universitário de Santiago, 3810-193 Aveiro, Portugal*
[c] *INESC TEC and Faculty of Engineering of the University of Porto, R. Dr. Roberto Frias, 4200-465 Porto, Portugal*
[d] *INESC-ID, Instituto Superior Técnico, University of Lisbon, Av. Rovisco Pais, 1, 1049-001 Lisbon, Portugal*

Abstract

In this paper an overloading prevention of a private customer power distribution transformer (PDT) in an island in Portugal through the means of a new smart electric vehicle (EV) charging scheduler is proposed. The aim of this paper is to assess the repercussion of the penetration of additional power to restore the full level of EV battery state of charge (SoC) on dielectric oil deterioration of the PDT of a private industry client. This will allow EVs to charge while their owners are at work at three different working shifts during the day. In addition, the system is part of an isolated electric grid in a Portuguese Island. A transformer thermal model is utilised in this paper to assess hot-spot temperature by having the information of the load ratio. The data used for the main inputs of the model are the private industry client daily load profile, PDT parameters, the characteristics of the factory and EV parameters. This paper demonstrates that the proposed solution allows avoiding the overloading of the PDT, thus mitigating the loss-of-life, while charging all the EVs plugged-in at the beginning of each working shift.

Keywords: Electric vehicle; battery SoC; insular grids; transformer thermal ageing; hot-spot temperature; electrical energy storage.

Nomenclature

d	The daily distance covered by an EV.
d_R	The maximum range of the EV.
E_i	The initial SOC of an EV battery.
g_r	Average winding to average oil (in tank) temperature gradient at rated current in K.
H	Hot-spot factor.
i_{P_T}	The total load current.
i_R	The rated current.
K	Load factor (load current/rated current).
k_{11}	Thermal model constant.
k_{21}	Thermal model constant.
k_{22}	Thermal model constant.
L	Loss of life.
L_L^T	Loading limit of the transformer.
N	Total number of time intervals.
n	Any given number.
P_{EV}	EV rated charging power in W.
P_f	Factory load in W.
P_r	Distribution transformer rated power in W.

* Corresponding author at the Faculty of Engineering of the University of Porto,
R. Dr. Roberto Frias, 4200-465 Porto, Portugal.
E-mail address: catalao@ubi.pt.

P_{sl}	A pre-set limit.
P_T	Total load in W.
P_Ω	The remaining EV load that is superior to the P_{sl}.
R	Ratio of load loss to no-load loss at rated current.
t	Period of the day in time units (h or min).
Δt_n	Time interval.
V	Relative ageing rate.
V_n	Relative ageing rate during interval n.
x	Exponential power of total losses versus top-oil (in tank) temperature rise (oil exponent).
y	Exponential power of current versus winding temperature rise (winding exponent).
τ_o	Average oil time constant.
τ_w	Winding time constant.
μ	The natural logarithmic mean.
σ	The standard deviation of the corresponding normal distribution.
Θ_a	The average ambient temperature in °C.
Θ_o	Top-oil temperature in °C.
$\Delta\Theta_{o,i}$	Top-oil (in tank) temperature rise at start in K.
$\Delta\Theta_{o,r}$	Top-oil temperature rise at rated current in K.
Θ_h	Winding hottest-spot temperature in °C.
$\Delta\Theta_{h,i}$	Hot-spot-to-top-oil (in tank) gradient at start in K.
$\Delta\Theta_{h,r}$	Hot–spot temperature rise at rated current in K.

Indices

a	Ambient Temperature
d	Domestic
EV	Electric Vehicle
f	Factory
h	Hot–spot
i	At start/initial
n	Index of the time interval
o	Top-oil
r	Rated Load
t	Period of the day index in time units [h or min].
w	Winding

Table of abbreviations

ACAP	Portuguese Automobile Association
DN	Distribution network
EU-27	European Union
EV	Electric vehicle
HMI	Human–machine interaction
LoL	Loss of life
ONAN	Oil natural air natural
PDF	Probability density function
PDT	Power distribution transformer

RES   Renewable energy sources
SG   Smart grid
SoC   State of charge
V2G   Vehicle-to-grid

1. Introduction

Nowadays mobility is ever more a central foundation for countless economic and private activities and as a consequence is an essential part of our life. On the other hand, mobility consumes more and more energy and leads to substantial environmental problems. More than 70% of the transport energy consumption in the European Union (EU-27) (2010) is consequently consumed by road traffic, and more than 90% of such type of energy consumption is based on the use of fossil fuels [1] [2]. Common concerns on the subject of urban air pollution, climate change, and dependence on expensive and unstable supplies of fossil fuels have lead researchers and policy makers to look for alternative choices besides to the traditional internal combustion petroleum-fuelled engine vehicles, such as EVs [3] [4]. Utilising only RES for charging has the potential to reduce the lifetime carbon dioxide emissions of an EV by at least 80% when compared with the average new vehicle with internal combustion engine [5] [6].

EV could bring various benefits, such as lower emissions of several air pollutants and noise, growing energy efficiency when compared to internal combustion engines, and the substitution of fuel as the main primary energy source for road transport [7] [8] [9]. A substantial widespread penetration of EVs could also have a great effect on the power system. The effects on the system peak load, power plant dispatch, and carbon emissions rely on both the power plant tools and the EVs charging mode [10].

The usual design horizons for power grids are dozens of years as a result of long service life of grid assets. EVs could produce new and unforeseen and sudden load patterns with possibly high simultaneity factors as a result of commuter traffic [10]. Additionally, with a rising number of EVs plugged to power systems for charging, there is also a preoccupation that the distribution networks (DN) already installed could turn out to be extra loaded than predicted compared with the time of their conception. Therefore, reduced implementation of EVs may well result in a reduced effect, however if the penetration total amount of EVs increases, a concrete possibility may occur of local DNs being congested [11] [12].

Many EVs charging at the same time could origin grid insufficiencies related with the available capacity and security [13]. Such events can be prevented, if they are correctly incorporated in the grid. If the EVs are operated accordingly – integrating them in the grid could be a substantial and important

occasion. Consequently, charging of a high quantity of EVs at the same time can be possible [14]. Devoid of such organised integration, the grid might suffer feeder congestions, excessive voltage drops, line overloads, etc.

Energy systems operation in isolated areas such as islands is often based on the highly costly importation of fossil fuels, which turns out to be a difficult problem with different ramifications including economic, environmental, and confidence of being constantly supplied, with the latest being especially significant for any isolated system such as islands [15] [16]. As a result, insular networks that present weaker structures than the mainland ones could be more seriously affected. It is necessary to supply all or at least the most part of the energy demand on site which usually are RES. The penetration of such systems in insular areas are central target of energy policies during the last few years and the design and structure of electric power grids will be forced to change considerably with the recent growing interest in RES [17].

A large shift from the traditional to a new smart grid (SG) networks was witnessed in the last few years. Such kind of transition is converted into an evolution from a typical radial energy flow to novel and systems with an increased complexity, but with better features such as a higher efficiency, a better incidence of distributed generation, better preservation of the environment, and greater reliability. The so called new paradigm of SG is outlining strategies to focus on the energetic needs of this century and afterwards, in order to accomplish such improvements [18]. The notion of SG is getting a noticeable role in both energy research and policy in the European Union [19]. The recent progress in SG research has predicted the connection of distributed RES and EVs to the power network and the numerous technical challenges that come from such a new paradigm and thus have to be approached properly [20].

The implementation of SG paradigm in insular areas has been increasing with the installation of diverse test systems in other islands around the world. Albeit the interconnected power system structure is deemed to be more rigid as regards to stability, isolated areas which could offer an essential foundation for potential islanding operation requirements could be seen as perfect testing grounds for the pre-evaluation of the SG paradigm [21].

The DN infrastructure is conceived to provide electricity to final clients and the planning is usually found on the assessed demand of electricity. For the abovementioned reason, there is a broad necessity to create modelling methods to assist the quantification of the impact that a great implementation level of

EVs could have on DNs and consequently guarantee that such ecologically positive technology is not needlessly constrained. As a result, the PDTs by being essential links in DNs will consequently begin to suffer exceptional loads from EV charging. A significant number of diverse research studies were recently released to evaluate if the current DN and fundamentally the global adoption of EVs could be tolerated by the transformer insulation temperature [12] [22] [23] [24] [25] [26] [27] [28] [29].

In [22] the control strategies that can eliminate or at least mitigate the hastened aging of a 25 kVA PDT that might be caused by load peaks instigated by EVs charging are implemented. Other study [23] deliberates how high implementation of EVs will greatly influence the development of home energy management and PDT systems with the intention of decreasing the effect of EV battery charging on PDTs by using real load consumption data from Austin, Texas, in the course of a characteristic summer day. In [24] is created a model to define the effect of large implementation rates of additional power to restore the full level of EV battery SoC on the dielectric oil deterioration of PDTs through UK generic low voltage DN model. In [12] a method is described for assessing the effect of EVs charging on overhead PDTs, also presenting a novel smart charging algorithm that regulates EVs charging based on assessed transformer temperatures. In [28] an analysis of the impacts of price-incentive based demand response on a neighbourhood PDT ageing has been performed through a MILP model of a neighbourhood composed of smart households with different end-user profiles. The impact of hybrid EVs on the life duration of the low-voltage/medium-voltage transformer utilising a thermal model to assess the Θ_h is studied in [30].

In [31] the impact of second generation EVs on the insulation life of the PDT by taking into account the time-of-use prices is investigated. In [32] EV charging is formulated as a receding horizon optimization problem that includes the present and anticipated constraints of the distribution network over a finite charging horizon. The impact of EVs charging on PDT overload and LoL in the presence of rooftop solar photovoltaic is probabilistically quantified in [33]. Finally, in [34] a model is created to determine the influence of simultaneous EV charging on the dielectric oil deterioration of two PDTs, one at a residential area and other at work.

A recent hot topic in research is the smart charging of EVs. The aim is to comprehend the necessary adaptation of the existing operational control mechanisms to implement the smart charging or to propose new ones. In [35] a double-layer smart charging management algorithm for EVs in working place parking lots considering SG concept is proposed. A probabilistic method which associates two unique datasets of

real world EV charging profiles and residential smart meter load demand in an urban and rural area in a heavily loaded UK distribution network is presented in [36]. In [37] is developed a smart charging framework to identify the benefits of non-residential EV charging to the load aggregators and the distribution grid. Whereas in [38] a smart management and scheduling model for large number of EVs parked in an urban parking lot is proposed. In [39] a campus based driver behaviour is gathered with face to face survey in Yildiz Technical University, Turkey and the survey data is utilised to determine daily optimum charging profile and increase the functionality of EVs. A part of the building energy management system algorithm for half-hourly vehicle-to-grid (V2G) capacity estimation using real-time EV scheduling is developed in [40]. Finally, in a novel design and implementation logic for a SG system that allows for dynamic interaction between EVs and the power grid is presented in [41].

In DNs one of the most common equipment that is found is the oil-immersed PDTs. For instance, distribution system of Azores uses almost exclusively oil-immersed PDTs with some of them upgraded not long ago [42]. Therefore, transformers in their current form are expected to stay operational for several years to come caused by its boundless utility with intrinsic high reliability and simplicity. As a result, the influence of characteristic SG operations for instance EV charging on transformer life and performance considerations must be properly evaluated.

This paper presents a model based on real data that allows the evaluation of the influence of additional power to restore the full level of EV battery SoC on the dielectric oil decay of an industry client PDT which in turn is a part of an isolated electrical grid of São Miguel Island, Azores, Portugal. The model takes into account the uncertainty of EV battery charging loads such as predictability of the EVs plug-in starting time, the battery SoC at the beginning and charging modes. Then, in order to mitigate the effect of the EVs on the loss-of-life (LoL) of the transformer, an overloading prevention by using the new smart EV charging scheduler is proposed and simulated. Hence, the novelty of this study consists in the proposal of a new EV charging scheduler used for a specific case of an island in a scenario with high penetration of EVs. The EVs charge at an industrial facility during three different shifts considering an industrial load.

This paper is organized as follows: in Section 2, the employed methodology is developed. Then, in Section 3, the DN of São Miguel, Azores, as well as the simulation results and critical analysis are presented and discussed. In Section 4 the overloading prevention of the industry client PDT through the

means of a model of a new smart EV charging scheduler is proposed and then the simulation results and critical analysis are presented and examined. Finally, the conclusions are drawn in Section 5.

2. Methodology

2.1 EV battery charging profiles

In a simplified way, the charging load of an EV is an addition to the existing load. EVs display remarkable differences when compared with other electrical loads due to their charging location being unpredictable. Three strategic factors exist which could affect the impact of EVs on DNs, specifically the features of additional power to restore the full level of EV battery SoC, the driving profile and electrical energy tariff incentives or other equivalent [29].

Throughout the time of the EV market growth, more and more car manufacturers enter the competition. As a consequence, a growing supply of EVs with different characteristics is available today [43]. As a result, in order to be more realistic, five different types of EVs are used in this study. The latest EV types including BMW i3, Renault ZOE, Nissan Leaf and Kia Soul are used for this study. Data for the charging types and duration of the five EVs are presented in Table 1 [44] [45] [46] [47].

<center>"Table 1 can be observed at the end of the document".</center>

BMW i3 percentage was selected in this study as high as 40% as it is the fastest selling EV in Portugal according to the ACAP – the Portuguese Automobile Association. Renault ZOE, Nissan Leaf and Kia Soul are assumed to have a 20% market penetration since these brands already appear to have a significant share in the EV market [48].

In the last few years, Lithium-ion (Li-ion) batteries have become widely utilised power source in manufacturing of EVs due to its high energy density, high power density and long lifetime [3]. Given their possibility to achieve higher specific energy and energy density, the implementation of Li-ion batteries is likely to increase quickly in the case of EVs. Approximately all EVs available in the market today use Li-ion batteries because of its mature technology. The capacity of a battery for light EVs is in the range of 6 kWh to 35 kWh. The charging time varies from 14 hours for slow charging batteries to less than an hour for fast charging batteries [43]. As a result of the fact that Li-ion batteries are the main option for the most recent group of EVs in development [24], in this paper it is anticipated that the considered EVs employ Li-ion batteries.

It is assumed that all the EVs making part of this case study have Li-ion batteries and in this study a simplified charging profile of such batteries is utilized. The aforementioned profile can be observed in Figure 1. When the battery SoC is reduced the charger functions at rated current, which allows a great percentage of the additional power to restore the full level of EV battery SoC being re-established throughout the initial hours of charging [49]. Figure 1 shows that the after the initial instants, the EV charges at constant current until the maximum battery voltage is reached, at that time the current falls while the EV charger preserves a constant voltage [26]. Usually, SoC is not only utilised to protect the battery from being overcharged or over discharged, but also to display the residual energy of the battery [50]. Also, for simplicity, the impact that the ambient temperature (Θ_a) could have on the additional power to restore the full level of EV battery SoC aspects is ignored and not considered for the considered case study.

"Figure 1 can be observed at the end of the document".

Additionally, the EV battery as soon as it begins charging until the battery reaches its full capacity is assumed to be continuous a charging process. The demand of the power throughout the entire charging process is frequently offered by the charging profile that could be different from vehicle to vehicle depending on battery charging mode and nature.

2.2 Model of EV Charging Load

For this study the typical EV Li-ion batteries charging profile is considered. Then, the stochastic behaviour of the starting SoC of the EV battery is assessed using a probability density function (PDF) related to travel distances. The additional power to restore the full level of EV battery SoC demand is given by the initial battery SoC, charging starting time and the characteristics of the battery. The SoC in this case study of an EV battery is determined by the travel habit of the EV user before plugging in for recharging and can be perceived as a random variable associated to the distance covered. The data for the model in this study is based on a Portuguese study of the general travel information regarding Portuguese drivers of conventional vehicles in 2011 in Lisbon area [51], as a consequence it is possible to generate the probability distribution of the quotidian travel distances as can be observed in Figure 2.

"Figure 2 can be observed at the end of the document".

Commonly it is considered that the distribution of the distance covered by the vehicle has a lognormal nature, with unexacting chances of manifestation of the negative distances, and a tail prolonging to

infinitum for positive distances [52]. The mathematical representation of the PDF of the EV travel distance is portrayed in the following equation (1):

$$(d;\mu,\sigma) = \frac{1}{d\sqrt{2\pi\sigma^2}} \times e^{-\frac{(\ln d - \mu)^2}{2\sigma^2}}, \, d > 0 \qquad (1)$$

where d defines the distance covered daily by a vehicle while μ represents mean and standard deviations of the normal distribution given by σ. In the case of the measurement taken from the vehicle travel distances from the aforementioned study in Portugal in 2011 as can be observed in Figure 2, $\mu = 2{,}995$ and $\sigma = 0{,}768$.

Once the average distance covered daily is set, the SoC at the start of a recharge cycle that is the remaining battery capacity can be portrayed utilising (1) by considering in this study that the SoC of an EV descents linearly with the journey distance (2):

$$E_i = \left(1 - \frac{d}{d_R}\right) \times 100 \, \% \qquad (2)$$

where E_i signifies the beginning SoC of an EV battery, the distance covered daily by an EV is d, which is a random variable conditioned to lognormal distribution and d_R represents maximum EV range and by considering that every trip is initiated with a SoC of 100%. A typical average value for the maximum travel distance for a conventional EV is 100 km [53].

Substituting (2) into (1) and switching the variable from d to E, the battery's SoC PDF once the journey of one day is accomplished is calculated through the following mathematical equation (3):

$$h(E;\mu,\sigma) = \frac{1}{d_R(1-E)\sqrt{2\pi\sigma^2}} \times e^{-\frac{[\ln(1-E)-(\mu-\ln d_R)]^2}{2\sigma^2}}, \, 0 < E < 1 \qquad (3)$$

and is plotted in Figure 3 truncated at 25% and 95% of battery SoC with parameters as in [54].

"Figure 3 can be observed at the end of the document".

Based on information withdrawn from both PDF, it is feasible to calculate the residual battery capacity at the beginning of each recharge cycle. In this paper the initial time of battery charging is influenced by the beginning of each working shift and the intention of the use of the EVs by the employees which is uncertain factor as seen in Figure 2.

2.3 Estimation of the Transformer Loss of Life (LoL)

In power systems a suitable conservation of mineral-oil-tilled PDTs is always particularly significant, as a result a necessity arose to adopt a serious methodology concerning transformer loading, with the aim to benefit as much as possible from their long duration service and availability. The isolation system of a PDT is essentially produced of oil and paper which will age. Sudden rise of the load causes a rise of the Θ_h and subsequently influences the thermal decomposition of the paper [55] [56] [57].

The hottest segment of the transformer is going to be the most damaged given that the temperature distribution does not follow a uniform profile. Therefore, the Θ_h directly affects the life duration of transformers [24] [30]. For the thermally upgraded paper the relative ageing rate is greater than a unity for Θ_h higher than 110 ºC and signifies that the dielectric oil ages sooner in relation with the acceleration of ageing at a standard Θ_h, and it is inferior than a unity for Θ_h lower than 110 ºC [12].

By designation, the Θ_h is the hottest temperature of any location in the transformer winding. By experiencing large electrical loads it creates high core-winding temperatures which in turn result in chemical breakdown of insulating oil and insulating paper [58].

The fundamental idea behind the top-oil temperature (Θ_o) rise model is that a rise of internal losses is seen as a result from an escalation in the PDT loading and consequently of total temperature inside of the transformer. As seen in C57.91-2011 standard [56] temperature oscillations depend on the PDT's overall thermal time constant that as a result relies on the heat transfer rate to the thermal capacity of the transformer and to the environment [58].

The Θ_o rise in steady state has a direct impact on the overall transformer internal losses, while the Θ_h is defined as a time function for a load current variable and Θ_a [55]. The dielectric oil inside of the operational PDT is vulnerable to all four categories of stresses – such as thermal, electrical, environmental and mechanical. The ageing of the dielectric oil of the PDT is influenced by the consequence of every stress factors or the interaction repercussion such factors [59].

In such cases or situations where increasing step of loads are verified, both the Θ_o and winding Θ_h rise to a value equivalent to load factor of K [55]. K defines the load factor and is represented by:

$$K = \frac{i_{P_T}}{i_R} \tag{4}$$

where i_{P_T} is the total load current and i_R is the rated current.

The mathematical representation of top-oil $\Theta_o(t)$ temperature is as follows (5):

$$\Theta_o(t) = \Delta\Theta_{o,i} + \left\{\Delta\Theta_{o,r} \times \left[\frac{1+R \times K^2}{1+R}\right]^x - \Delta\Theta_{o,i}\right\} \times \left(1 - e^{-t/(k_{11} \times \tau_o)}\right) \tag{5}$$

where the top - oil temperature increase at start is represented by $\Delta\Theta_{o,i}$ in °K while $\Delta\Theta_{o,r}$ represents the top - oil temperature increase at rated current, the load loss to no-load loss ratio is defined by R, x is the oil exponent, k_{11} expresses one of the thermal model constants and finally the average oil time constant is represented by τ_0 [55].

The mathematical expression of the hot-spot temperature rise $\Delta\Theta_h(t)$ is as follows (6):

$$\Delta\Theta_h(t) = \Delta\Theta_{h,i} + \left\{H \times g_r \times K^y - \Delta\Theta_{h,i}\right\} \times \left[k_{21} \times \left(1 - e^{-t/(k_{22} \times \tau_w)}\right) - (k_{21} - 1) \times \left(1 - e^{-(t \times k_{22})/\tau_o}\right)\right] \tag{6}$$

where $\Delta\Theta_{h,i}$ is the hot-spot-to-top-oil gradient at the start while y defines the winding exponent as for the av. winding to av. oil is represented by g_r, hot-spot factor is expressed by H, k_{21} and k_{22} represent the other thermal model constants and finally the winding time constant is defined τ_w.

For the situations and cases of declining step of loads, as seen in the literature depicted before, the Θ_o and winding Θ_h diminishes to a level given by K [55]. Top - oil temperature $\Theta_o(t)$ is considered as follows (7):

$$\Theta_o(t) = \Delta\Theta_{o,r} \times \left[\frac{1+R \times K^2}{1+R}\right]^x + \left\{\Delta\Theta_{o,i} - \Delta\Theta_{o,r} \times \left[\frac{1+R \times K^2}{1+R}\right]^x\right\} \times \left(e^{-t/(k_{11} \times \tau_o)}\right) \tag{7}$$

The mathematical expression of the hot-spot temperature rise is as follows (8):

$$\Delta\Theta_h(t) = H \times g_r \times K^y \tag{8}$$

At long last, according to the standard in [55] with $\Theta_o(t)$ and $\Delta\Theta_h(t)$ from Eq. (5) and (6) in case of growing load steps, and Eq. (7) and (8) in case of declining load steps and plus the Θ_a the general and complete hot-spot temperature $\Theta_h(t)$ expression is mathematically represented as follows (9):

$$\Theta_h(t) = \Theta_a + \Theta_o(t) + \Delta\Theta_h(t) \tag{9}$$

The ageing rate V [56] corresponds to the decay of paper isolation for which a Θ_h is decreased or increased when related with ageing rate at standard Θ_h (110ºC) [55]. The relative ageing rate V, as seen in the IEC 60076-7 standard [55], in case of thermally upgraded paper is (10):

$$V = e^{\left(\frac{15000}{110+273} - \frac{15000}{\Theta_h+273}\right)} \tag{10}$$

Completed a given interval of time, the LoL expression L for the duration of the time period t_n is represented in the following equation (11):

$$L = \int_{t_1}^{t_2} V dt \quad \text{or} \quad L \approx \sum_{n=1}^{N} V_n \times t_n \tag{11}$$

To discover the transient solutions for Θ_o and Θ_h – a thermal model is generated and proposed for the PDT as in [29].

The properties of the PDT on which this paper is based are withdrawn from Ravetta et al. [60] that presented the data of a real 250 kVA oil transformer with Oil Natural Air Natural (ONAN) cooling where a natural convectional flow of hot oil is utilized for cooling. The properties are given in Table 2.

"Table 2 can be observed at the end of the document".

3. Case Study

3.1 Structural elements of the insular grid

The Azores, a Portuguese autonomous region, is an archipelago located in the North Atlantic and comprises 9 islands. São Miguel Island is the main one, having around 140,000 inhabitants and covers 760 km² [29].

In this study, a part of São Miguel medium voltage DN was used as an example. A transformer that supplies a private industry client was selected. Figure 4 shows a part of the medium voltage DN and an identification of several outputs. For this case study the transformer substation PT1094 was utilised which supplies one private industry client via a 250kVA, 10kV/0.4kV oil-immersed transformer. Figure 5 shows a simplified layout of the analysed low voltage (LV) grid.

"Figure 4 can be observed at the end of the document".

"Figure 5 can be observed at the end of the document".

Private industry client consists of a factory that manufactures sugar out of sugar beet. It employs circa 120 workers and operates in 3 working shifts of 8 hours each. The first working shift begins at 08:00, the second at 16:00 and the third at 00:00. It is assumed in this paper that the workers are distributed all over the working shifts equally.

For the duration of a few days of February 2014 several measurements were performed at the transformer substation PT1094 and the energy consumption of industry client was recorded, thus a daily

baseline load profile was created as shown in Figure 6. The data collected from the measurements are provided under the SiNGULAR project [61]. It is also given the power factor of the transformer – approximately 0.95. It may be observed that a 250 kVA transformer is correctly sized for a 140 kW of peak in daily baseline load profile, considering that a typical value for an inferior size transformer would be 167 kVA which is not adequate [42].

<p align="center">"Figure 6 can be observed at the end of the document".</p>

Despite the fact that early sales of EVs have been solid, presently they represent just 0.02% of the total value of light vehicle sales in Portugal. However, there are substantial increase prospects till 2020 [62]. Regardless of such numbers, in this study, higher penetration levels are examined. Principally for an insular area, for example São Miguel, the relatively high transportation cost of fossil fuels, the presence of rich potential of RES, and the opportunities that could spawn from the efficient management of an EV fleet [21], lead the authors to believe that the penetration levels that are likely to be met in such areas in the future will be significantly higher than in continental areas. In addition, state driven incentives typically have a tendency to aim preferably areas such as islands and as a result, eventual subsidiary programs or tax reduction plans to encourage the acquisition and use of EVs are to be expected to greatly persuade customers to substitute their traditional vehicle with an EV.

3.2 Simulation Results

By taking into consideration the data collected from the PDF it the transformer thermal model can be applied by using the load ratio as an input to obtain the Θ_h and Θ_o temperatures. The total load $P_T(t)$ (in kW) on the transformer is the sum of the factory load P_f and loading from n_{EV} randomly selected EVs (12):

$$P_T(t) = \left| P_f(t) + \sum_{EV=1}^{n_{EV}} P_{EV}(t) \right| \tag{12}$$

For this case study one day of the baseline load profile of the month of February of the transformer substation PT1094 is used and two different scenarios are examined.

3.2.1 Scenario 1

In the first scenario different penetration ratios of EVs for each working shift are simulated for this factory, beginning with 40% penetration and then with 45%, 50%, 55%, and 60%. The aforementioned particular percentages are set as such due to the reason of being just under and/or above the transformer

loading limit, other percentages are redundant. Lastly, it is assumed that the EVs are plugged-in or start to charge at the beginning of each working shift.

The outcome on the daily baseline load profile of the transformer substation PT1094 generated by the energy consumption of the EVs at several penetration ratios from the first scenario is shown in Figure 7. The daily baseline load profile is also displayed as 0% penetration ratio.

By observing Figure 7 it can be perceived that for a penetration of EVs of more than 40% the PDT is overloaded. Additionally, from the information acquired from the model and presented in Figure 7, it is possible to calculate the transformer insulation ageing affected by the Θ_h which is presented in Figure 8 and then to calculate LoL at the designated penetration ratios of the transformer. The LoL of the transformer can be observed in percentage and in hours and minutes for each day of EV charging which means that from the transformer expected life at 0% penetration is subtracted the number of minutes or hours for each day of charging. The results can be seen in the Table 3.

"Figure 7 can be observed at the end of the document".

"Figure 8 can be observed at the end of the document".

"Table 3 can be observed at the end of the document".

3.2.2 Scenario 2

The second scenario comprises the following elements: all EVs are charged with fast charging mode starting with 15% penetration and then with 20%, 25%, 30%, and 35%. The same percentages are set as the preceding scenario with the purpose of observing the difference between slow and fast charging modes. In the same manner as in the previous scenario, it is assumed that the workers plug-in their EVs to charge at the beginning of each working shift.

The consequence on daily baseline load profile of PT109 transformer substation generated by the energy consumption of the EVs at several penetration ratios from the second scenario is shown in Figure 9.

Through the analysis of Figure 9 it can be noticed that for a penetration of EVs of more than 15% the PDT is deeply overloaded and as much as at inferior penetration ratios it is overloaded. Likewise, from the information acquired from the model and presented in Figure 9, it can be calculated the transformer insulation ageing determined by the Θ_h which is presented in Figure 10. By the use of the ageing

equations (9) and (10), transformer LoL of the transformer can now be determined. The results can also be observed in the Table 3.

"Figure 9 can be observed at the end of the document".

"Figure 10 can be observed at the end of the document".

3.3 Critical Analysis

By analysing the results acquired from Table 3 it can be inferred that the transformer LoL is only affected after a penetration of a certain number of EVs which is relatively high. If the EV owners make such profile of charging a routine the transformer will have a deteriorating LoL after some time.

The contrast of both scenarios at 35% EV penetration in the Figures 11 and 12 highlights the level of impact in the transformer ageing by using fast charging over slow charging. Through the analysis of both Figures 7 to 10 and Table 3 it can be concluded that each beginning of a shift will influence employees to favour the first hour of charging, that will produce a concentration of EVs charging simultaneously which in turn could originate an overloading of the PDT, a sudden increase of the Θ_h and thus will affect the transformer lifetime.

"Figure 11 can be observed at the end of the document".

"Figure 12 can be observed at the end of the document".

By observing the first scenario it can be concluded that for more than 40% of EV penetration the transformer will be overloaded resulting in an increase of the Θ_h of the PDT. The LoL slightly increases with the increase of EV penetration in this scenario.

In an unlikely event of the second scenario boing put in practice, the LoL of the PDT is meaningfully higher. As a result, it is advised to refrain from the fast charging mode since the slow mode takes at maximum 5 hours which is always less than a working shift of 8 hours and consequently all the workers will have the batteries of their EVs charged by the end of their working shift.

4. The solution of the transformer overloading – new smart EV charging scheduler

Given the overload that the transformer suffers at the beginning of each working shift, the authors propose a solution through a scheduler. The solution consists of a model that evaluates the effect of EVs charging loads on the ageing of a real PDT that supplies the private industry client, and then schedules the charging of EVs in an optimal manner that allows avoiding the overloading of the transformer. The

rescheduling process purpose is to charge the batteries of all the EVs in a timely manner meanwhile avoiding the overloading of the transformer.

4.1 The Smart Charging Scheduler's architecture

Initially, a pre-set limit (P_{sl}) of the permissible load has to be introduced in the scheduler in order to limit the sum of the factory loading and the EV batteries. P_{sl} can be less or equal than 95% of the transformer's loading limit (L_L^T) so that at least 5% of the transformer capacity remains unused in order to always have a certain reserve. P_{sl} at 95% is expressed by:

$$P_{sl} \leq L_L^T \times 0.95 \tag{13}$$

The operation of such device consists of collecting the data of the transformer parameters, EVs batteries SoC, the industry client load and the Θ_a and then to reschedule the charging of EVs that surpass the P_{sl} of the scheduler. Such device will also have a data logger and HMI (human–machine interaction) device in order to display all the information related to the made recordings and the modelled data and also to allow an interactive use of the device with functions such as the easy setting of a new P_{sl}. Finally the scheduler will have a wireless transmitter in order to send the information to an exterior platform so it could be accessed everywhere by all sorts of portable devices. The operation of the proposed scheduler is displayed in Figure 13.

"Figure 13 can be observed at the end of the document".

As seen before, $P_T(t)$ is the sum of the loads of the factory and EVs. On the other hand, let the $P_\Omega(t)$ be the remaining EV load that is superior to the P_{sl} in any given instant t (14):

$$P_\Omega(t) = \begin{cases} 0, & \forall\ P_T(t) \leq P_{sl} \\ P_T(t) - P_{sl}, & \forall\ P_T(t) > P_{sl} \end{cases} \tag{14}$$

Thus, the new EV charging scheduler operates in the following mode: at first a charging time frame is established, then effectuates readings of the DN data, the number of charging EVs and their charging characteristics, such as the type of charging and how much SoC the recently connected EV has. The scheduler also reads the factory load and Θ_a, and finally assesses the Θ_h and LoL. Immediately after this operation it verifies if P_T is equal or higher than P_{sl}. If this is the case, then the scheduler is activated and the remaining EV load P_Ω is rescheduled to the next charging time frame which in this case study is 15 minutes.

The total load P_T of the succeeding time frame $(t+1)$ is represented by:

$$P_T(t+1) = \begin{cases} \left| P_f(t+1) + \sum_{EV=1}^{n_{EV}} P_{EV}(t+1) \right| & , \; \forall \, P_T(t) \leq P_{sl} \\ \left| P_f(t+1) + \sum_{EV=1}^{n_{EV}} P_{EV}(t+1) + P_\Omega(t) \right| & , \; \forall \, P_T(t) > P_{sl} \end{cases} \tag{15}$$

which in turn becomes the following equation:

$$P_T(t+1) = \begin{cases} P_T(t+1) & , \; \forall \, P_T(t) \leq P_{sl} \\ P_T(t+1) + P_\Omega(t) & , \; \forall \, P_T(t) > P_{sl} \end{cases} \tag{16}$$

Finally, if all the EVs are charged then the scheduler is put in stand-by until a new EV connects. The detailed operation of the new EV charging scheduler is shown in Figure 14 through the means of a flowchart.

"Figure 14 can be observed at the end of the document".

4.2 Simulation Results

4.2.1 Scenario 1

After the implementation of the new EV scheduler model several simulations were performed and several results were obtained and analysed which are subject to various comparisons. In case of a slow charging mode Figure 15 shows how the scheduler prevents the overloading of the transformer when compared with Figure 7 at several penetration ratios, up to 60%. A small improvement was verified of the Θ_h in comparison with the first scenario seen in Section 3 through the comparison between Figures 8 and 16. In Figure 16, when comparing both scheduling and non-scheduling solutions regarding the peak values a slight improvement can be observed.

"Figure 15 can be observed at the end of the document".

"Figure 16 can be observed at the end of the document".

The results in how much LoL was saved in relation with the scenario without the EV charging scheduler is shown in Table 4. The values of LoL observed in the table show that the LoL per day is gradually increasing as the number of EV penetration increases as well. Juxtaposition between the rescheduled charging of EVs at 60% penetration and non-scheduled charging can be seen in Figure 17. A small improvement of Θ_h is verified by using the scheduler. This improvement presented in Figure 18 corresponds to saving 7.54% of the LoL of that day.

"Figure 17 can be observed at the end of the document".

"Figure 18 can be observed at the end of the document".

"Table 4 can be observed at the end of the document".

The next step after the aforementioned simulations were concluded was to simulate scenarios with high penetration of EVs, as much as 60%, and at different pre-set limits. The results show that the EVs are always charged until the end of each working shift, in point of fact nowhere near the end of the shift, but three to four hours earlier. The results can be seen in Figure 19 for the daily load profile and Figure 20 for the Θ_h. By means of the ageing equations V and L, the LoL of the transformer can now be determined. The results show that the LoL decreases each time the P_{sl} is set lower and can be seen in the Table 5.

"Figure 19 can be observed at the end of the document".

"Figure 20 can be observed at the end of the document".

"Table 5 can be observed at the end of the document".

With the intention of testing the limits an extreme event was also simulated in order to assess until what point the EV charging scheduler is viable. In this figure, a large improvement can be observed when comparing both scheduling and non-scheduling solutions regarding the peak values. The results show that at an EV penetration ratio of 100% and a P_{sl} of 75% the EVs are all charged before the working shift ends as it can be observed in Figure 21 for the daily load profile. In Figure 22 can be noticed the quantification of saved LoL in relation with the scenario without the new EV charging scheduler by comparing the Θ_h. Yet in this case is witnessed a large improvement of LoL, 76.76% of LoL of that day is saved. Such an outcome is presented in Figure 22 by observing the Θ_h curves.

"Figure 21 can be observed at the end of the document".

"Figure 22 can be observed at the end of the document".

4.2.2 Scenario 2

The second scenario consists in an unlikely event of all EVs being charged with fast charging mode at a 35% penetration. Just as in the previous scenario, it is assumed that the workers plug-in their EVs to charge at the beginning of each working shift. After the implementation of the new EV scheduler model a simulation was performed and results were obtained. A large improvement was verified of the Θ_h in comparison with the second scenario seen in Section 3. A comparison between the rescheduled charging of EVs at 35% penetration and non-scheduled charging can be seen in Figure 23. In this figure, a large improvement can be witnessed when comparing both scheduling and non-scheduling solutions in terms of

peak values. Figure 24 shows how much LoL was saved in relation with the scenario without the new EV charging scheduler through means of Θ_h. As much as 98.08% of LoL was saved by using the EV charging scheduler. Even if using the fast changing mode the results demonstrate that the EVs are always charged until the end of each working shift, in actual fact considerably far from the end of each shift.

"Figure 23 can be observed at the end of the document".

"Figure 24 can be observed at the end of the document".

4.3 Critical Analysis

By deciding for the new EV charging scheduler the factory employees and personnel can always be assured that their personal EVs will be charged at the ending of each working shift under a plethora of circumstances. Even in such extreme scenarios in which all the connected EVs are charged employing the fast charging mode at a 35% EV penetration the scheduler can operate so that all the EVs will be fully charged at the end of the working shift. Such a solution also allows the charging of all the EVs without crossing the loading limit of the transformer and in the end the solution permits the saving of transformer's useful life. Even by varying the P_{sl} the results show that the LoL decreases each time the P_{sl} is set lower.

5. Conclusion

In this paper a case study of an overloading prevention of an industry client PDT in an island in Portugal employing a new smart EV charging scheduler was proposed. At first, the model that assessed the additional power to restore the full level of EV battery SoC impact on the insulation ageing of a real PDT at a private industry client was applied and described. Different charging scenarios with several penetration ratios were studied at three different working shifts. Since transformer insulation ageing is mainly influenced by the Θ_h, a transformer thermal model was considered in estimating Θ_h for a specific load ratio. Thermal ageing was then calculated and analysed. Given the fact that the 250 kVA transformer has a significant capacity to be used for a side activity – this study showed that even though it has, it still can be overloaded after a certain increase of EV penetration. In face of the overload that the transformer suffers at the beginning of each working shift, a novel schedule solution was proposed which consists of a model that makes the evaluation of the influence of additional power to restore the full level of EV battery SoC on the insulation decay of a real PDT, and then scheduled the charging of the EV in an

optimal manner that turned possible to avoid the overloading of the studied transformer through the development of the new smart EV scheduler. Such a solution also allowed the charging of all the EVs without crossing the loading limit of the transformer and, in the end, the solution allows saving of transformer's useful life, which is an important contribution towards sustainability. The verified improvement of Θ_h by using the scheduler is measured through saved LoL percentage per day and ranges between 7.54% at 60% EV penetration and 95% P_{sl} and 76.76% at 100% EV penetration and 75% P_{sl}. Even in extreme cases in which the fast changing mode is employed the results show that the EVs are always scheduled to fully charge until the end of each working shift without overloading the PDT. As much as 98.08% of LoL was saved by using the EV charging scheduler.

Acknowledgements

Bibliography

[1] Z. Dimitrova and F. Maréchal, "Techno–economic design of hybrid electric vehicles and possibilities of the multi-objective optimization structure," *Applied Energy,* vol. 161, pp. 746-759, 2016.

[2] H. Helms, C. Kämper and U. Lambrecht, "2 - Carbon dioxide and consumption reduction through electric vehicles," in *Advances in Battery Technologies for Electric Vehicles*, Woodhead Publishing, 2015, pp. 17-34.

[3] J. Jaguemont, L. Boulon and Y. Dubé, "A comprehensive review of lithium-ion batteries used in hybrid and electric vehicles at cold temperatures," *Applied Energy,* vol. 164, pp. 99-114, 2016.

[4] E. Xydas, C. Marmaras, L. M. Cipcigan, N. Jenkins, S. Carroll and M. Barker, "A data-driven approach for characterising the charging demand of electric vehicles: A UK case study," *Applied Energy,* vol. 162, pp. 763-771, 2016.

[5] A. Schuller, C. M. Flath and S. Gottwalt, "Quantifying load flexibility of electric vehicles for renewable energy integration," *Applied Energy,* vol. 151, pp. 335-344, 2015.

[6] R. Nealer, D. Reichmuth and D. Anair, "Cleaner Cars from Cradle to Grave - How Electric Cars Beat Gasoline Cars on Lifetime Global Warming Emissions," Union of Concerned Scientists, Cambridge, MA, 2015.

[7] T. Donateo, F. Licci, A. D'Elia, G. Colangelo, D. Laforgia and F. Ciancarelli, "Evaluation of emissions of CO2 and air pollutants from electric vehicles in Italian cities," *Applied Energy,* vol. 157, pp. 675-687, 2015.

[8] B. Yagcitekin, M. Uzunoglu and A. Karakaş, "A new deployment method for electric vehicle charging infrastructure," *Turkish Journal of Electrical Engineering & Computer Sciences,* vol. 24, pp. 1292-1305, 2016.

[9] B. Yagcitekin, M. Uzunoglu, A. Karakas and O. Erdinc, "Assessment of electrically-driven vehicles in terms of emission impacts and energy requirements: a case study for Istanbul," *Journal of Cleaner Production,* vol. 96, pp. 486-492, 2015.

[10] F. Salah, J. P. Ilg, C. M. Flath, H. Basse and C. v. Dinther, "Impact of electric vehicles on distribution substations: A Swiss case study," *Applied Energy,* vol. 137, pp. 88-96, 2015.

[11] M. Noori, Y. Zhao, N. C. Onat, S. Gardner and O. Tatari, "Light-duty electric vehicles to improve the integrity of the electricity grid through Vehicle-to-Grid technology: Analysis of regional net revenue and emissions savings," *Applied Energy,* vol. 168, pp. 146-158, 2016.

[12] A. Hilshey, P. Hines, P. Rezaei and J. Dowds, "Estimating the Impact of Electric Vehicle Smart Charging on Distribution Transformer Aging," *IEEE Transactions on Smart Grid,* vol. 4, no. 2, pp. 905-913, 2013.

[13] B. Yagcitekin, M. Uzunoglu, A. Karakas and M. Vurgun, "Assessment of a car park with electric vehicles," in *2013 Fourth International Conference on Power Engineering, Energy and Electrical Drives (POWERENG)*, Istanbul, 2013.

[14] R. Das, K. Thirugnanam, P. Kumar, R. Lavudiya and M. Singh, "Mathematical Modeling for Economic Evaluation of Electric Vehicle to Smart Grid Interaction," *IEEE Transactions on Smart Grid,* vol. 5, no. 2, pp. 712-721, 2014.

[15] P. Kadurek, "São Miguel Island as a case study on a possible usage of Electric vehicle to store energy," *World Electric Vehicle Journal,* vol. 3, no. 4, pp. 756-763, 2009.

[16] E. Rodrigues, R. Godina, S. Santos, A. Bizuayehu, J. Contreras and J. Catalão, "Energy storage systems supporting increased penetration of renewables in islanded systems," *Energy,* vol. 75, pp. 265-280, 2014.

[17] O. Erdinc, N. G. Paterakis and J. P. Catalão, "Overview of insular power systems under increasing penetration of renewable energy sources: Opportunities and challenges," *Renewable and Sustainable Energy Reviews,* vol. 52, pp. 333-346, 2015.

[18] J. S. Vardakas, N. Zorba and C. V. Verikoukis, "Power demand control scenarios for smart grid applications with finite number of appliances," *Applied Energy,* vol. 162, pp. 83-98, 2016.

[19] I. Colak, G. Fulli, S. Sagiroglu, M. Yesilbudak and C.-F. Covrig, "Smart grid projects in Europe: Current status, maturity and future scenarios," *Applied Energy,* vol. 152, pp. 58-70, 2015.

[20] M. B. Toft, G. Schuitema and J. Thøgersen, "Responsible technology acceptance: Model development and application to consumer acceptance of Smart Grid technology," *Applied Energy,* vol. 134, pp. 392-400, 2014.

[21] O. Erdinc and N. G. Paterakis, "Chapter 1 - Overview of Insular Power Systems: Challenges and Opportunities," in *Smart and Sustainable Power Systems: Operations, Planning and Economics of Insular Electricity Grids*, J. Catalão, Ed., Boca Raton, Florida, CRC Press (TAYLOR & FRANCIS Group), 2015.

[22] Q. Gong, S. Midlam-Mohler, E. Serra, V. Marano and G. Rizzoni, "PEV Charging Control Considering Transformer Life and Experimental Validation of a 25 kVA Distribution Transformer," *IEEE Transactions on Smart Grid,* vol. 6, no. 2, pp. 648-656, 2015.

[23] R. Vicini, O. Micheloud, H. Kumar and A. Kwasinski, "Transformer and home energy management systems to lessen electrical vehicle impact on the grid," *IET Generation, Transmission & Distribution,* vol. 6, no. 12, pp. 1202-1208, 2012.

[24] K. Qian, C. Zhou and Y. Yuan, "Impacts of high penetration level of fully electric vehicles charging loads on the thermal ageing of power transformers," *International Journal of Electrical Power & Energy Systems,* vol. 65, pp. 102-112, 2015.

[25] Q. Gong, S. Midlam-Mohler, V. Marano and G. Rizzoni, "Study of PEV Charging on Residential Distribution Transformer Life," *IEEE Transactions on Smart Grid,* vol. 3, no. 1, pp. 404-412, 2012.

[26] M. J. Rutherford and V. Yousefzadeh, "The Impact of Electric Vehicle Battery Charging on Distribution Transformers," in *2011 Twenty-Sixth Annual IEEE Applied Power Electronics Conference and Exposition (APEC)*, Fort Worth, TX, USA, 2011.

[27] R. Godina, N. Paterakis, O. Erdinc, E. Rodrigues and J. Catalão, "Electric vehicles home charging impact on a distribution transformer in a Portuguese island," in *2015 International Symposium on Smart Electric Distribution Systems and Technologies — EDST 2015*, Vienna, 2015.

[28] N. Paterakis, I. Pappi, O. Erdinc, R. Godina, E. Rodrigues and J. Catalão, "Consideration of the impacts of a smart neighborhood load on transformer ageing," *IEEE Transactions on Smart Grid,* 2016.

[29] R. Godina, N. Paterakis, O. Erdinc, E. Rodrigues and J. Catalão, "Impact of EV charging-at-work on an industrial client distribution transformer in a Portuguese island," in *2015 Australasian Universities Power Engineering Conference (AUPEC)*, Wollongong, Australia, 2015.

[30] H. Turker, S. Bacha, D. Chatroux and A. Hably, "Low-Voltage Transformer Loss-of-Life Assessments for a High Penetration of Plug-In Hybrid Electric Vehicles (PHEVs)," *IEEE Transactions on Power Delivery,* vol. 27, no. 3, pp. 1323-1331, 2012.

[31] Y. O. Assolami and W. G. Morsi, "Impact of Second-Generation Plug-In Battery Electric Vehicles on the Aging of Distribution Transformers Considering TOU Prices," *IEEE Transactions on Sustainable Energy,* vol. 6, no. 4, pp. 1606-1614, 2015.

[32] J. d. Hoog, T. Alpcan, M. Brazil, D. A. Thomas and I. Mareels, "Optimal Charging of Electric Vehicles Taking Distribution Network Constraints Into Account," *IEEE Transactions on Power Systems,* vol. 30, no. 1, pp. 365-375, 2015.

[33] S. F. Abdelsamad, W. G. Morsi and T. S. Sidhu, "Probabilistic Impact of Transportation Electrification on the Loss-of-Life of Distribution Transformers in the Presence of Rooftop Solar Photovoltaic," *IEEE Transactions on Sustainable Energy,* vol. 6, no. 4, pp. 1565-1573, 2015.

[34] R. Godina, E. Rodrigues, N. Paterakis, O. Erdinc and J. Catalão, "Innovative impact assessment of electric vehicles charging loads on distribution transformers using real data," *Energy Conversion and Management,* vol. 120, pp. 206-216, 2016.

[35] B. Yagcitekin and M. Uzunoglu, "A double-layer smart charging strategy of electric vehicles taking routing and charge scheduling into account," *Applied Energy,* vol. 167, pp. 407-419, 2016.

[36] M. Neaimeh, R. Wardle, A. M. Jenkins, J. Yi, G. Hill, P. F. Lyons, Y. Hübner, P. T. Blythe and P. C. Taylor, "A probabilistic approach to combining smart meter and electric vehicle charging data to investigate distribution network impacts," *Applied Energy,* vol. 157, pp. 688-698, 2015.

[37] E. C. Kara, J. S. Macdonald, D. Black, M. Bérges, G. Hug and S. Kiliccote, "Estimating the benefits of electric vehicle smart charging at non-residential locations: A data-driven approach," *Applied Energy,* vol. 155, pp. 515-525, 2015.

[38] M. Honarmand, A. Zakariazadeh and S. Jadid, "Optimal scheduling of electric vehicles in an intelligent parking lot considering vehicle-to-grid concept and battery condition," *Energy,* vol. 65, pp. 572-579, 2014.

[39] B. Yagcitekin, M. Uzunoglu and A. Karakas, "A Charging Management of Electric Vehicles Based on Campus Survey Data," *Applied Mechanics and Materials,* vol. 492, pp. 43-48, 2014.

[40] K. N. Kumar, B. Sivaneasan, P. H. Cheah, P. L. So and D. Z. W. Wang, "V2G Capacity Estimation Using Dynamic EV Scheduling," *IEEE Transactions on Smart Grid,* vol. 5, no. 2, pp. 1051-1060, 2014.

[41] R. Abousleiman and R. Scholer, "Smart Charging: System Design and Implementation for Interaction Between Plug-in Electric Vehicles and the Power Grid," *IEEE Transactions on Transportation Electrification,* vol. 1, no. 1, pp. 18-25, 2015.

[42] EDA S.A. - Electricidade dos Açores, "Caracterização Das Redes De Transporte E Distribuição De Energia Eléctrica Da Região Autónoma Dos Açores," Ponta Delgada, 2014.

[43] K. Young, C. Wang, L. Y. Wang and K. Strunz, "Chapter 2 - Electric Vehicle Battery Technologies," in *Electric Vehicle Integration into Modern Power Networks*, New York, Springer New York, 2013, pp. 15-56.

[44] Bayerische Motoren Werke, "The new BMW i3 - Launches November 2013.," BMW UK, Printed in the UK, 2013.

[45] Kia Motors Europe, "The new Kia," Kia Motors Europe, Frankfurt am Main, Germany .

[46] Renault S.A., "Renault ZOE Simply Revolutionary," Renault U.K. Limited Customer Relations, The Rivers Office Park, Denham Way, Maple Cross, Rickmansworth, Hertfordshire, 2013.

[47] ©2014 Nissan North America, Inc. , "2014 Nissan Leaf Brochure," Dealer E-Process, 2014.

[48] ACAP, "Associação Automóvel de Portugal," [Online]. Available: http://www.acap.pt/pt/home. [Accessed 20 02 2015].

[49] J. Jaguemont, L. Boulon and Y. Dubé, "A comprehensive review of lithium-ion batteries used in hybrid and electric vehicles at cold temperatures," *Applied Energy,* vol. 164, pp. 99-114, 164.

[50] F. Yang, Y. Xing, D. Wang and K.-L. Tsui, "A comparative study of three model-based algorithms for estimating state-of-charge of lithium-ion batteries under a new combined dynamic loading profile," *Applied Energy,* vol. 164, p. 387–399, 2016.

[51] N. B. R. d. C. Pereira, Eficiência energética no sector dos transportes rodoviários: metodologia para quantificação do excesso de energia consumida devido ao factor comportamental na condução de veículos automóveis ligeiros, Lisbon: Departamento de Ciências e Tecnologia da Biomassa - Universidade Nova de Lisboa, 2011.

[52] P. Zhang, K. Qian, C. Zhou, B. Stewart and D. Hepburn, "A Methodology for Optimization of Power Systems Demand Due to Electric Vehicle Charging Load," *IEEE Transactions on Power Systems,* vol. 27, no. 3, pp. 1628-1636, 2012.

[53] K. Qian, C. Zhou, M. Allan and Y. Yuan, "Modeling of Load Demand Due to EV Battery Charging in Distribution Systems," *IEEE Transactions on Power Systems,* vol. 26, no. 2, pp. 802-810, 2011.

[54] S. I. Vagropoulos and A. G. Bakirtzis, "Optimal Bidding Strategy for Electric Vehicle Aggregators in Electricity Markets," *IEEE Transactions on Power Systems,* vol. 28, no. 4, pp. 4031-4041, 2013.

[55] IEC 60076-7, "Loading Guide for Oil-immersed Power Transformers," 2005.

[56] C57.91-2011, "IEEE Guide for Loading Mineral-Oil-Immersed Transformers and Step-Voltage Regulators," IEEE Standard, 2012.

[57] H. Pezeshki, P. Wolfs and G. Ledwich, "Impact of High PV Penetration on Distribution Transformer Insulation Life," *IEEE Transactions on Power Delivery,* vol. 29, no. 3, pp. 1212-1220, 2014.

[58] M. J. Heathcote, J & P Transformer Book, Oxford: Newnes, 2007.

[59] R. Godina, E. Rodrigues, J. Matias and J. Catalão, "Effect of loads and other key factors on oil-transformers ageing: sustainability benefits and challenges," *Energies,* vol. 8, no. 10, pp. 12147-12186, 2015.

[60] C. Ravetta, M. Samanna', A. Stucchi and A. Bossi, "Thermal behavior of distribution transformers in summertime and severe loading conditions," in *19th International Conference on Electricity Distribution*, Vienna, 2007.

[61] SiNGULAR, "Smart and Sustainable Insular Electricity Grids Under Large-Scale Renewable Integration," Grant Agreement No: 309048, FP7-EU, 2015. [Online]. Available: http://www.singular-fp7.eu/home/. [Accessed 2015].

[62] International Energy Agency, "Global EV Outlook - Understanding the Electric Vehicle Landscape to 2020," Similar Blue, Paris, 2013.

Tables

EVs	Ref	% of EV	Slow Charge		Fast Charge	
			Power kW	Time h	Power kW	Time h
BMW i3	[44]	40%	7.4	3	50	30m-1h
Renault ZOE	[46]	20%	7.4	3	43	30m-1h
Nissan Leaf	[47]	20%	6.6	5	44	30m-1h
Kia Soul	[45]	20%	6.6	4-5	50	30m-1h

Table 1 – Charging Types and Duration of the 4 EVs chosen for this study

Symbol		Case Study	Units
g_r	Average winding to average oil temperature gradient at rated current	15.9	Ws/K
H	Hot-spot factor	1.25	
k_{11}	Thermal model constant.	0.5	
k_{21}	Thermal model constant.	2	
k_{22}	Thermal model constant.	2	
P_r	Distribution Transformer Rated Power	250	kVA
R	Ratio of load loss to no-load loss at rated current	5.957	
x	Exponential power of total losses versus top-oil temperature rise	0.8	
y	Exponential power of current versus winding temperature rise	1.3	
$\Delta\Theta_{o,r}$	Top-oil temperature rise at rated current	41.5	K
τ_0	Average oil time constant	210	Minutes
τ_w	Winding time constant	10	Minutes

Table 2 – The Transformer Parameters used in this study

Scenario 1			Scenario 2		
EV Penetration	LoL (t)	LoL %	EV Penetration	LoL (t)	LoL %
40%	31 min	0.0003	15%	0h 33m	0.0003
45%	40 min	0.0004	20%	1h 20m	0.0007
50%	41 min	0.0004	25%	3h 19m	0.0019
55%	58 min	0.0005	30%	15h 11m	0.0084
60%	61 min	0.0006	35%	57h 12m	0.0318

Table 3 – LoL per Day of the Transformer due to EV Charging for both scenarios

EV Penetration	LoL (t)	LoL %
40%	39.16 min	0.0004
45%	49.74 min	0.0005
50%	52.12 min	0.0005
55%	53.28 min	0.0005
60%	71.54 min	0.0006

Table 4 – LoL per Day of the Transformer due to EV Charging

P_{sl} limits	LoL (t)	LoL %
70%	36.11 min	0.0003
75%	39.91 min	0.0004
80%	44.09 min	0.0004
90%	53.46 min	0.0005
95%	59.64 min	0.0006

Table 5 – LoL per Day of the Transformer due to EV Charging

Figures
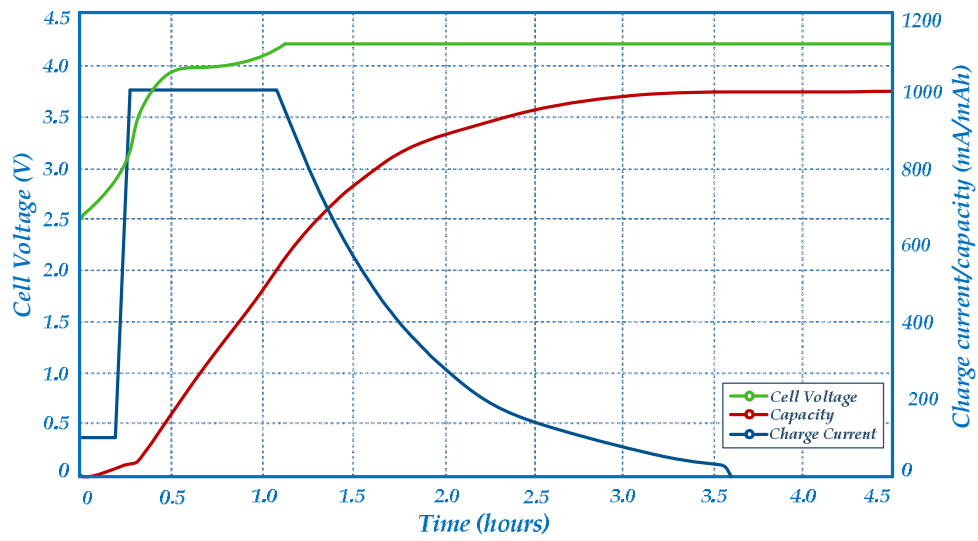
Figure 1 - The simplified charging profile of Li-ion batteries utilized in the study.
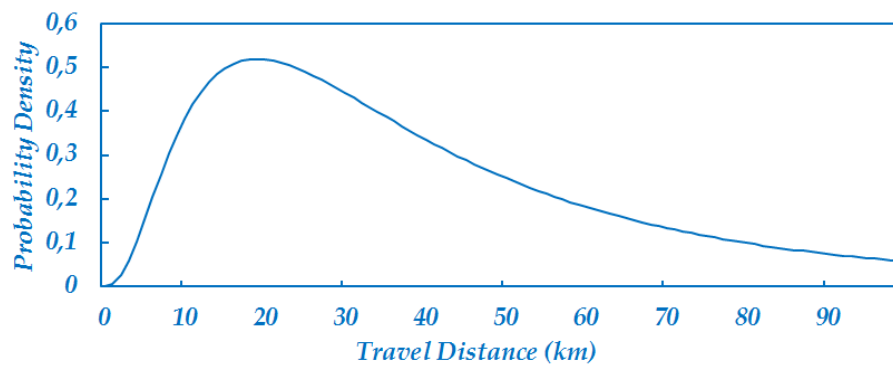
Figure 2 - PDF of quotidian vehicle travel distance.
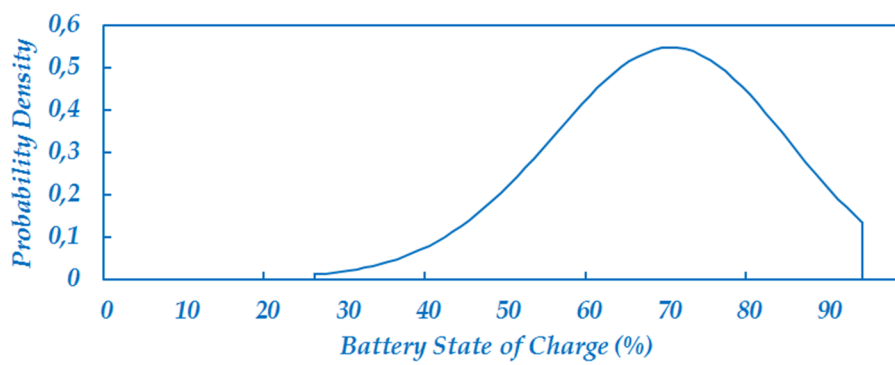
Figure 3 - PDF of battery SOC after one day of driving.

Figure 4 - A part of São Miguel medium voltage DN and the identification of PT1094 transformer

station [42].

Figure 5 - LV grid simplified layout.
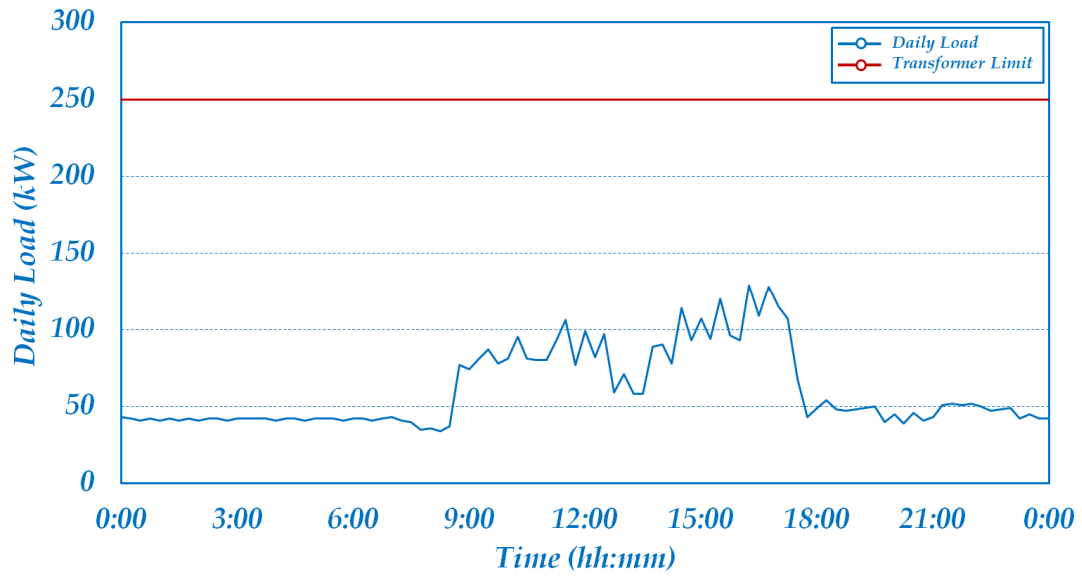
Figure 6 - The daily baseline load profile of the transformer substation PT1094.
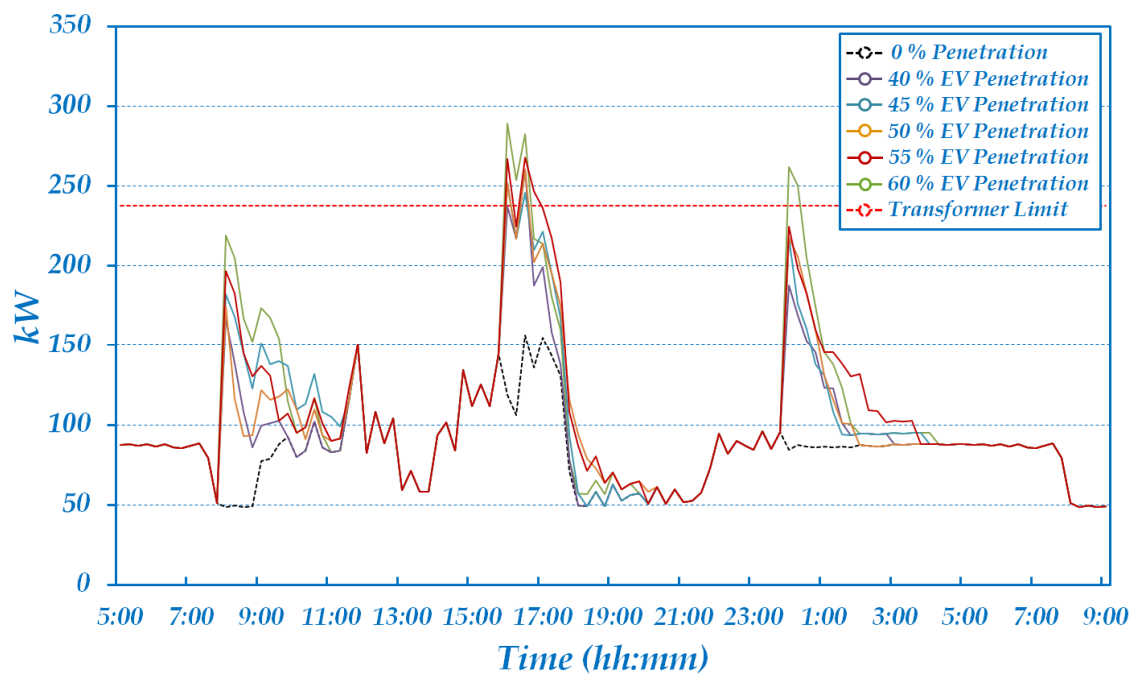
Figure 7 - The daily baseline load profile with the first scenario studied.
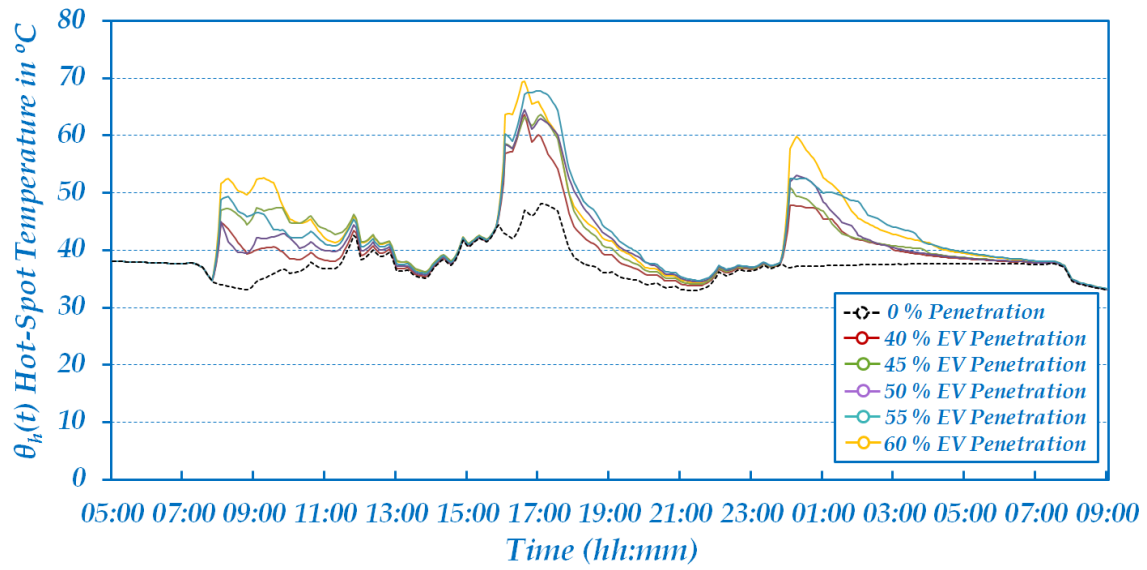
Figure 8 - Θ_h temperature of the distribution transformer in Scenario 1.
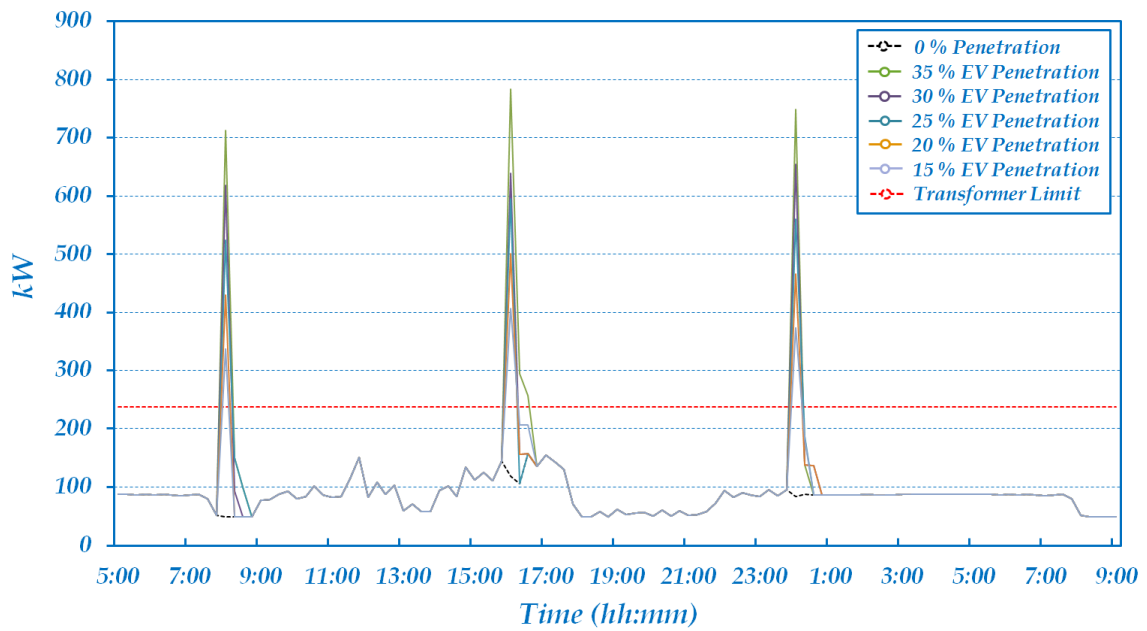
Figure 9 - The daily baseline load profile with the second scenario studied.
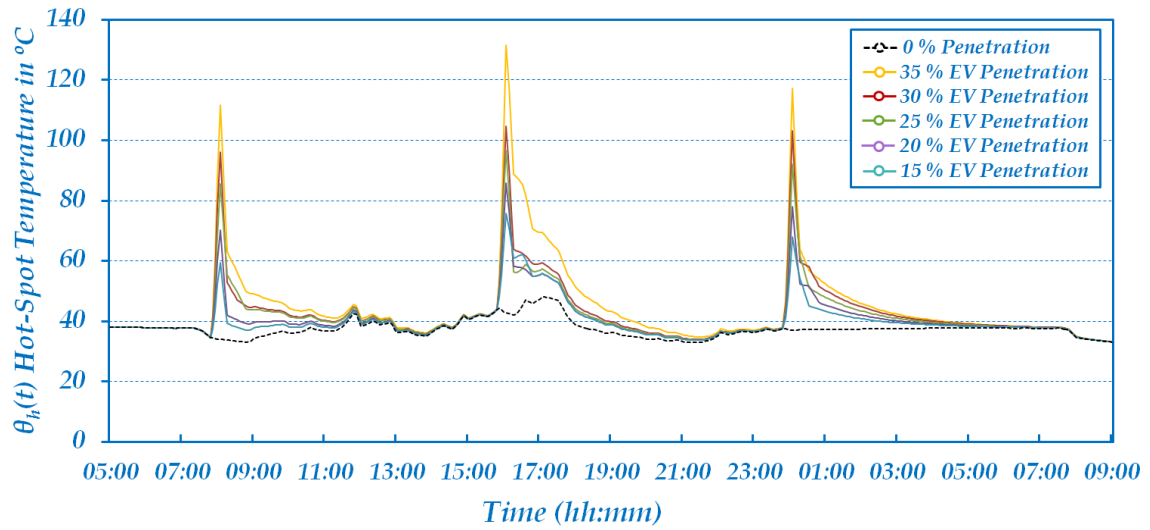
Figure 10 - Θ_h temperature of the distribution transformer in Scenario 2.
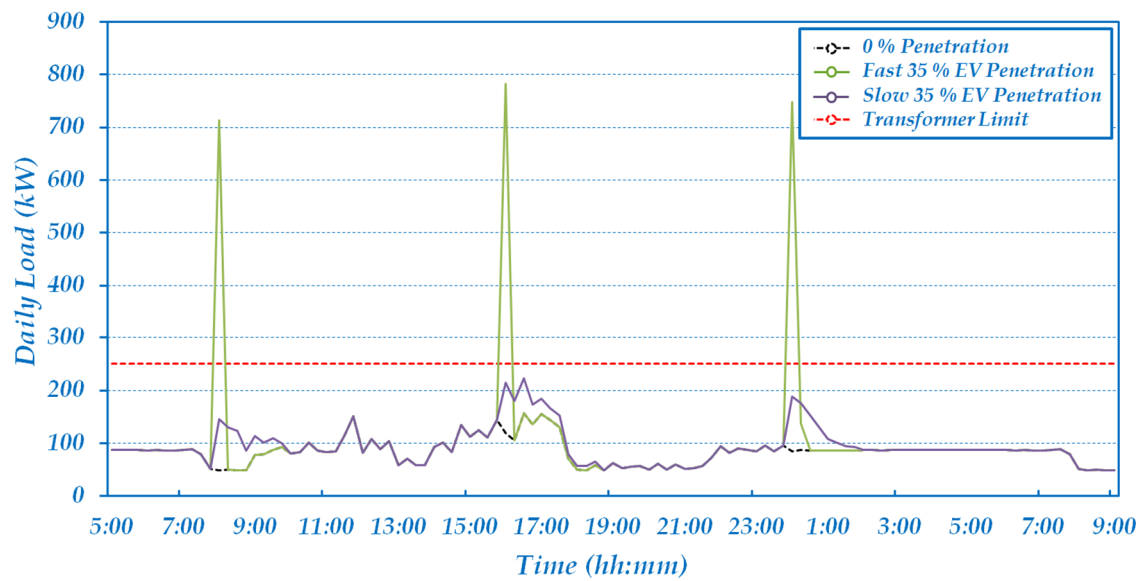
Figure 11 – Comparison of the daily baseline load profile of both slow and fast charging modes.
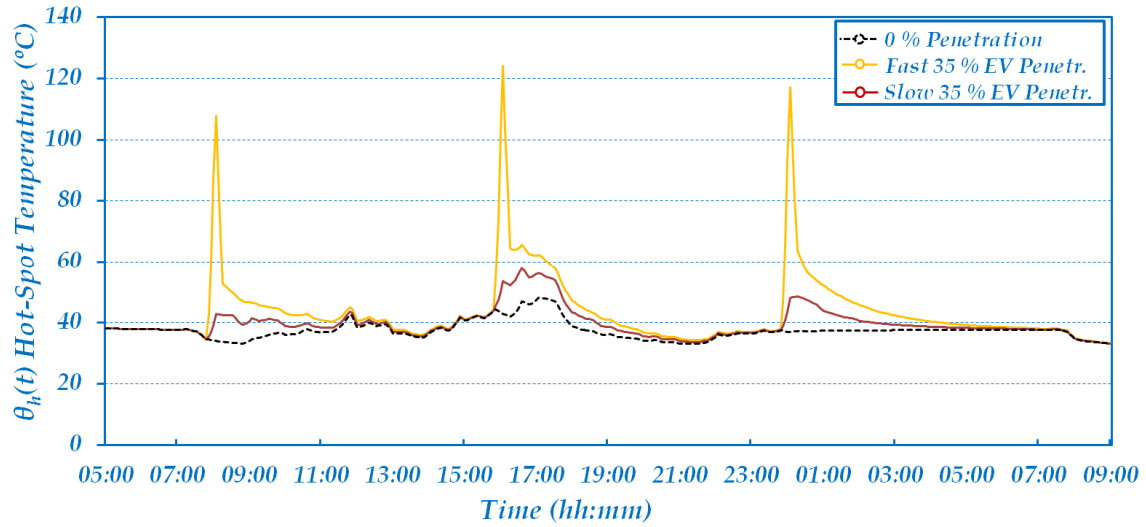
Figure 12 – Comparison of Θ_h temperature of the distribution transformer of both slow and fast charging modes.
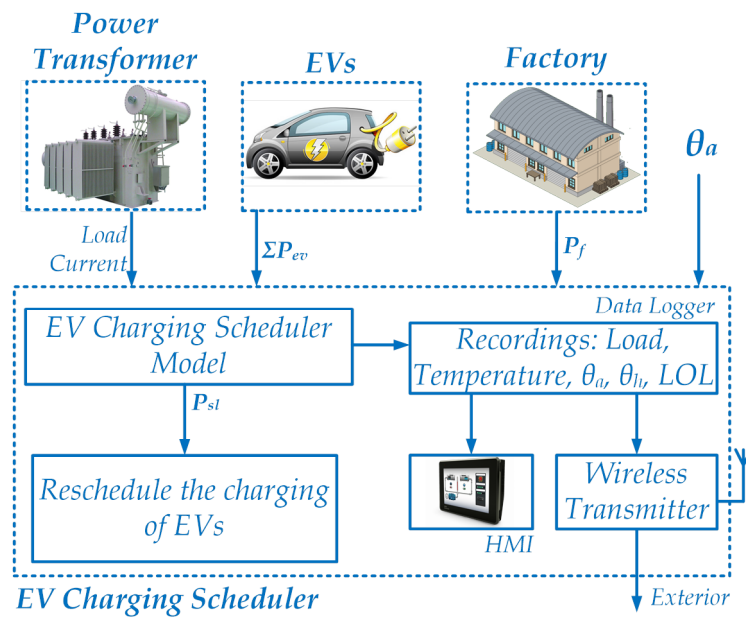
Figure 13 – The basic operation schematic of the EV Charging Scheduler.

Start

The Charging Time
Frame is Set

Read Distribution Network Data
Read EV Charging Characteristics
Read the Factory Load and Θ_a

Calculate Θ_h and LoL
Display Information

Are any EVs
charging ? — No

Yes

$P_T > P_{sl}$

Yes — No

Calculate P_σ

All EVs are
charged ? — Yes

No

Charging Time Frame
Charge until P_{sl}

Charging Time Frame

$P_\sigma + P_T > P_{sl}$ — Yes

No

All EVs are
charged ? — Yes

No

Charging Time Frame

End

Figure 14 – Detailed Scheduler Operation Flowchart.
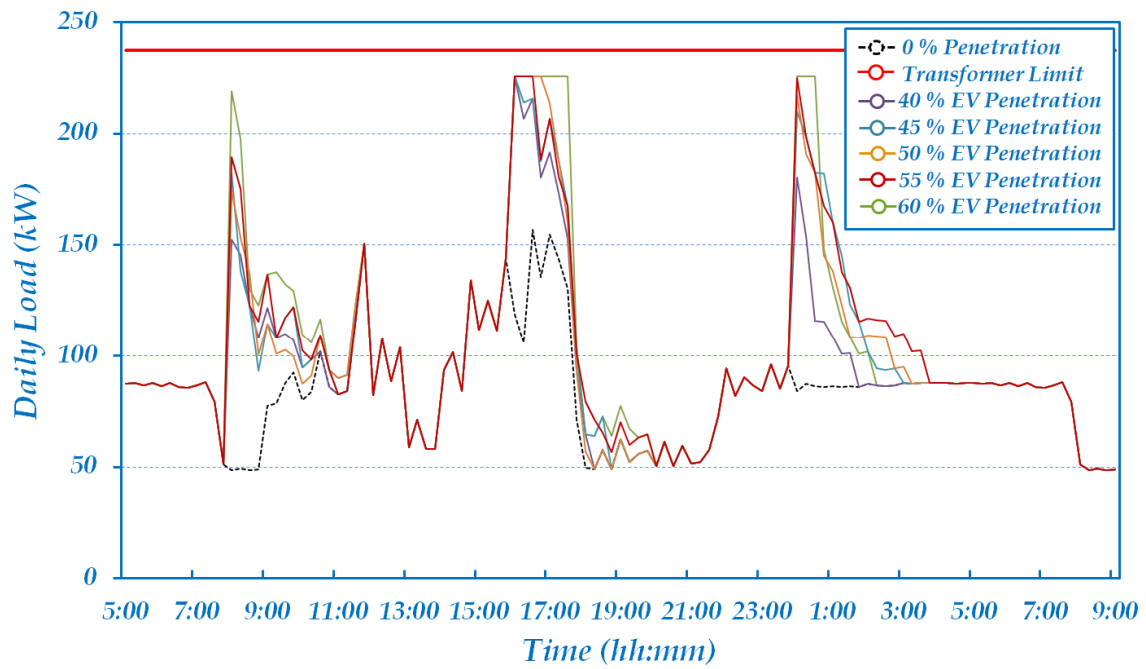
Figure 15 – The daily baseline load profile in slow charging mode with the Scheduler in operation.
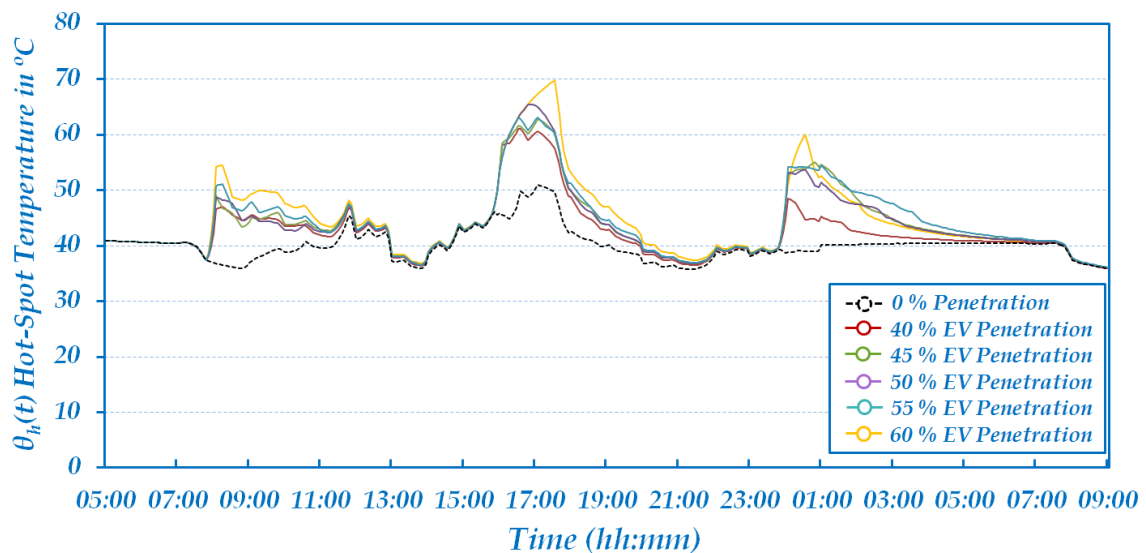
Figure 16 – The Θ_h Temperature in slow charging mode with the Scheduler in operation.
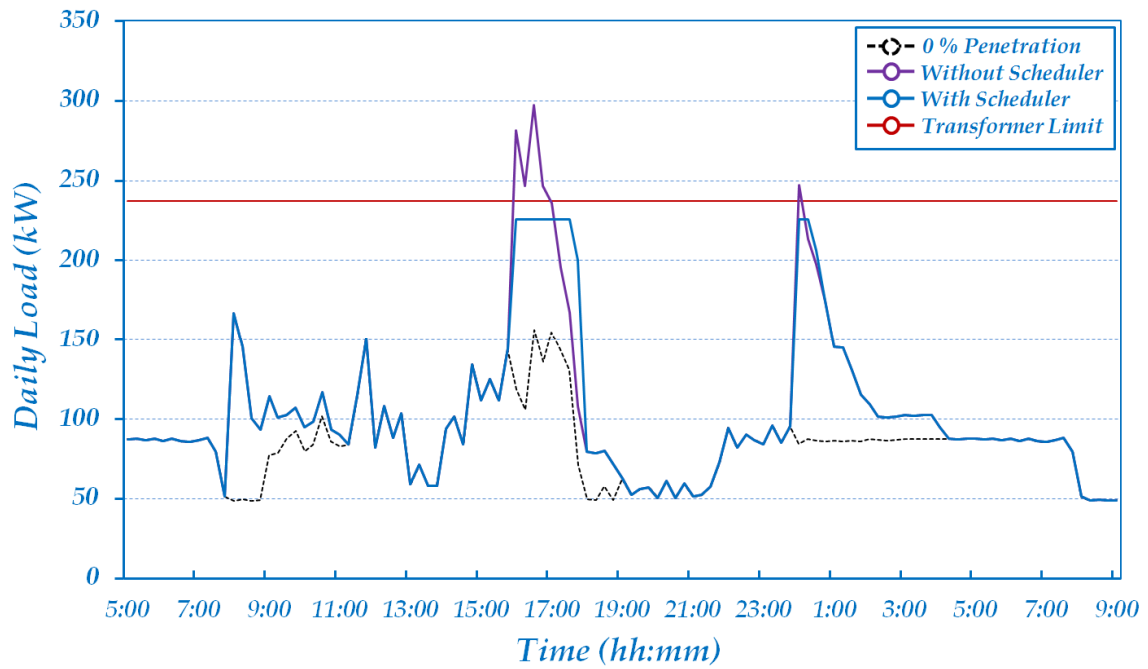
Figure 17 – Comparison in slow EV charging mode between the cases with the scheduler and without it at 60% EV penetration.
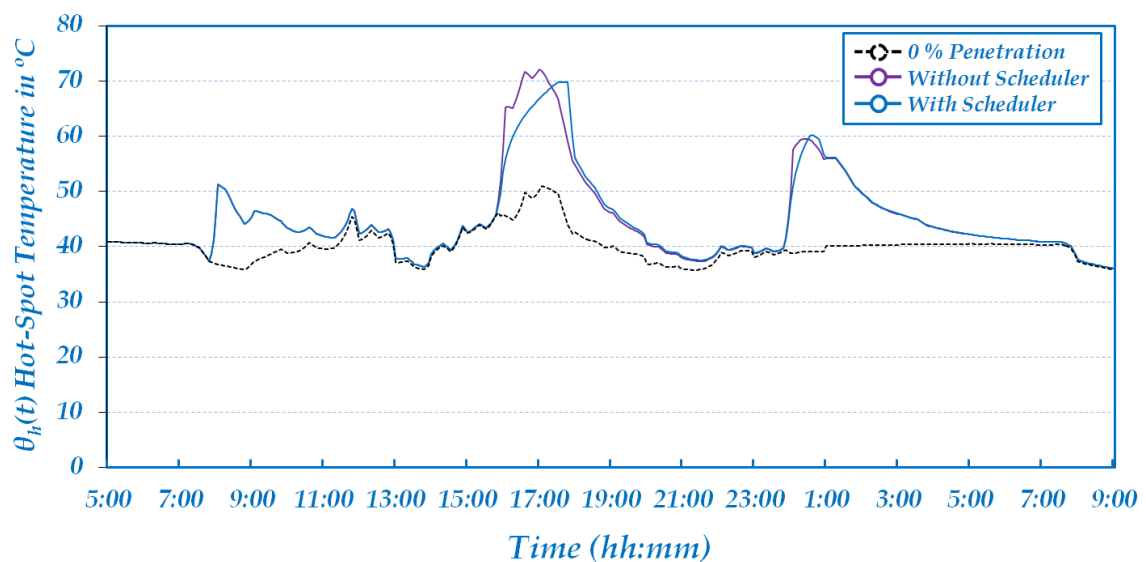
Figure 18 – Comparison of Θ_h between the cases with the scheduler and without it at 60% EV penetration.
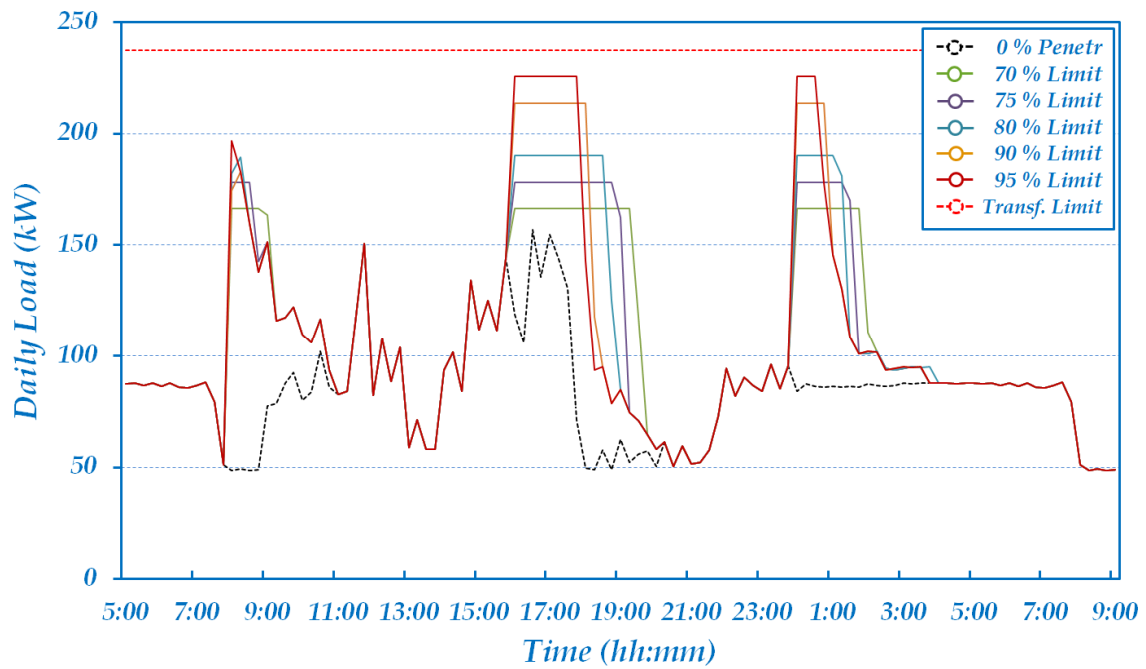
Figure 19 – Difference between the operations of the scheduler at several pre-set limits at a 60% penetration.
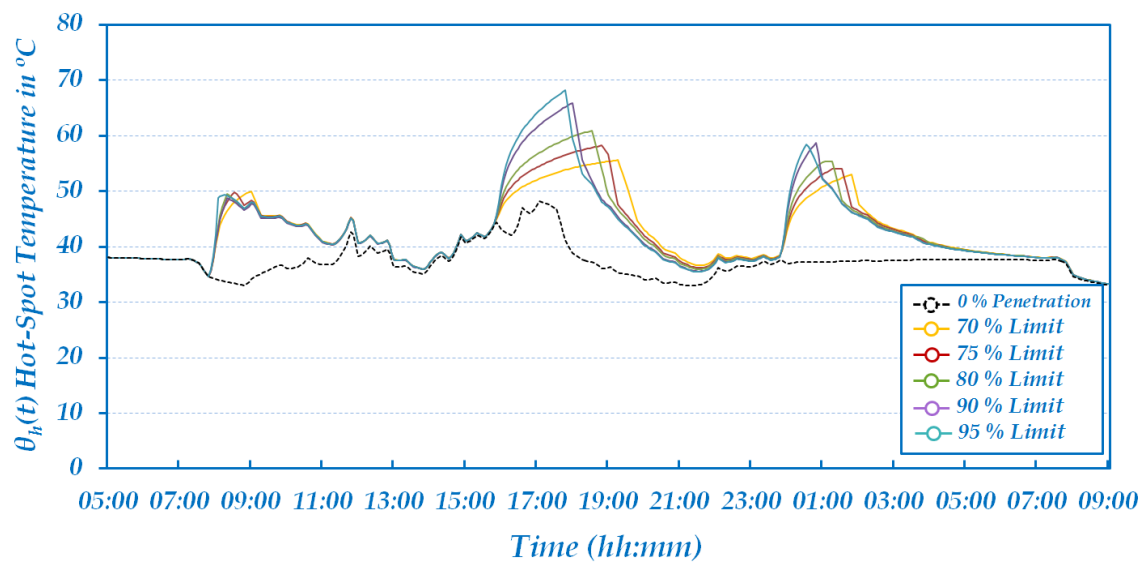
Figure 20 – Difference between the Θ_h at several scheduler pre-set limits at a 60% penetration.
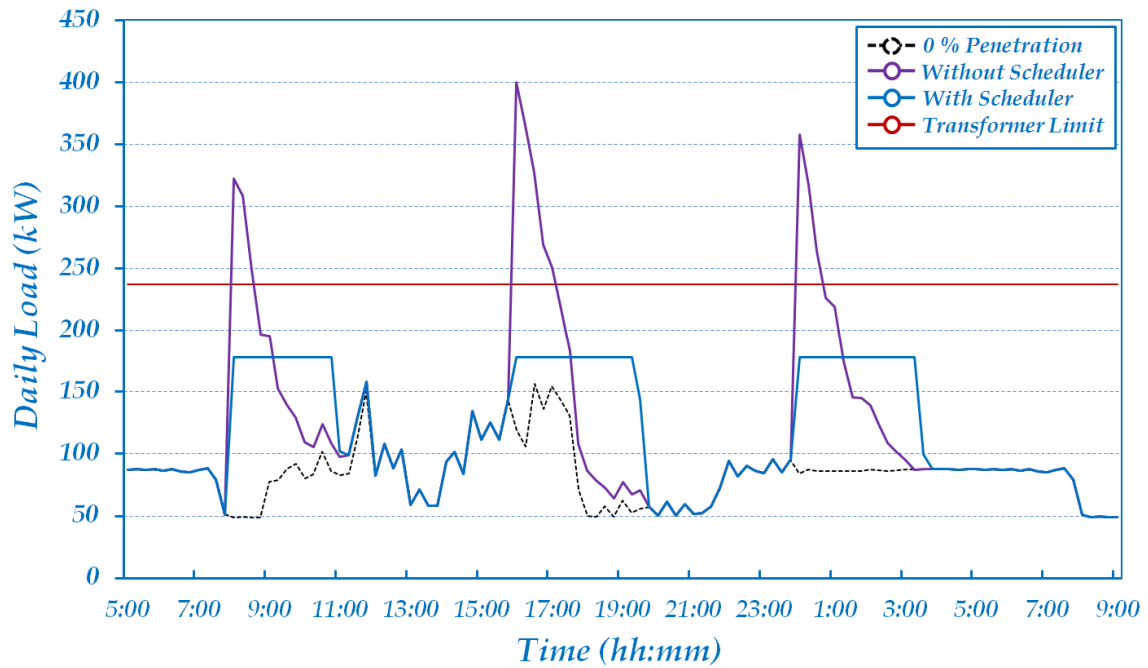
Figure 21 – Comparison of an extreme case with 100% EV Penetration with a scheduler at 75% limit or
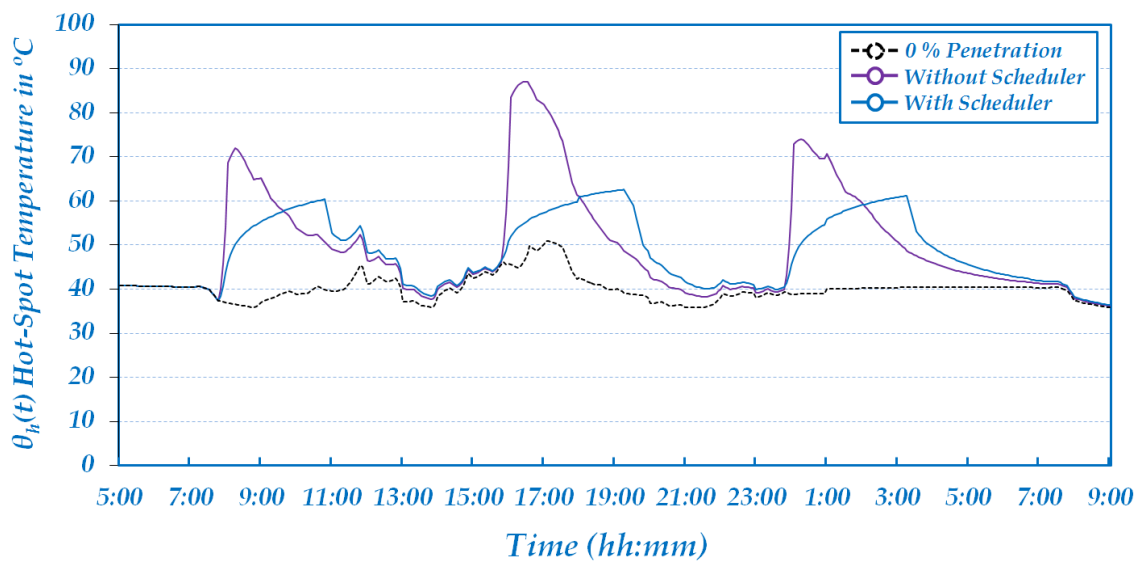
without it.

Figure 22 – Comparison of Θ_h of an extreme case with 100% EV Penetration with a scheduler at 75%
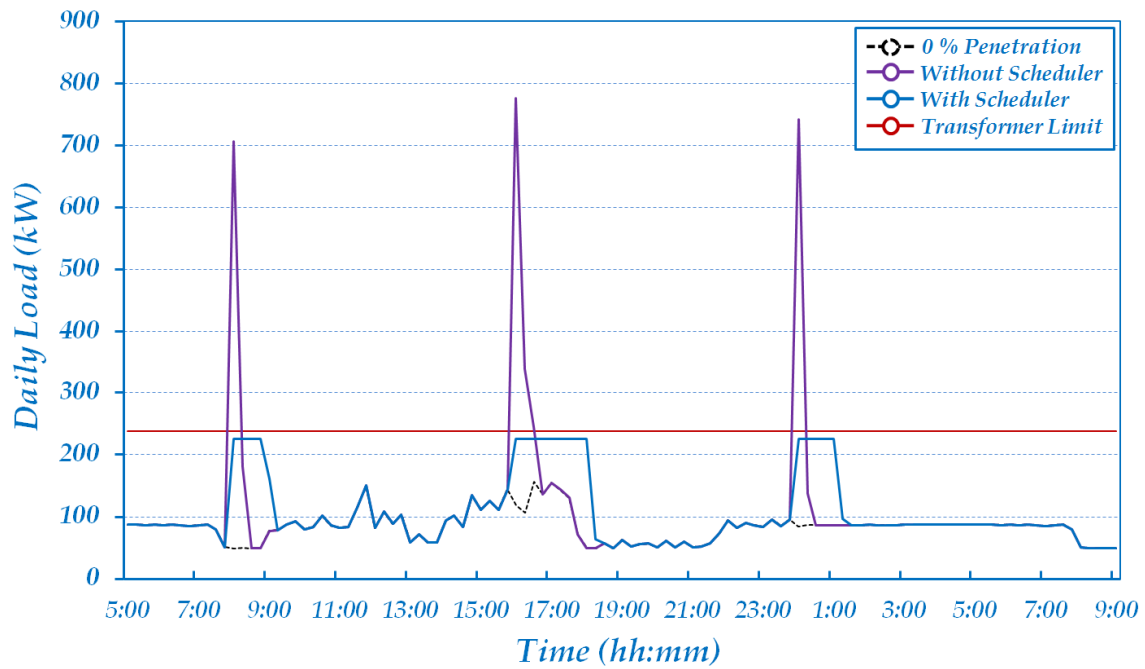
limit or without it.

Figure 23 – Comparison in fast charging mode of an extreme case with 35% EV Penetration with a scheduler at 95% limit or without it.
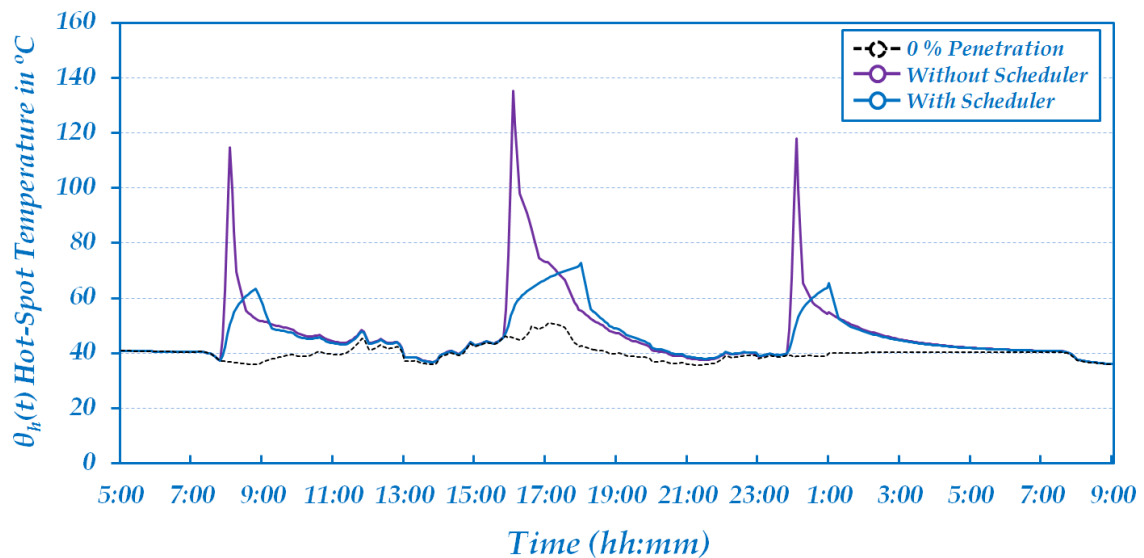

Figure 24 – Comparison in fast charging mode of Θ_h of an extreme case with 35% EV Penetration with a scheduler at 95% limit or without it.